ScientificScholar®
Knowledge is power
Publisher of Scientific Journals

www.surgicalneurologyint.com

Surgical Neurology International

Editor-in-Chief: Nancy E. Epstein, MD, Professor of Clinical Neurosurgery, School of Medicine, State U. of NY at Stony Brook.

SNI: Neuro-Oncology

Editor
Mitsutoshi Nakada, MD
Kanazawa University, Ishikawa, Japan

SNI
Open Access

Original Article

Advanced magnetic resonance imaging for glioblastoma: Oncology-radiology integration

Abdulsalam Mohammed Aleid, Abdulrahim Saleh Alrasheed, Saud Nayef Aldanyowi, Sami Fadhel Almalki

Department of Surgery, College of Medicine, King Faisal University, AlAhsa, Saudi Arabia.

E-mail: Abdulsalam Mohammed Aleid - 225094489@student.kfu.edu.sa; Abdulrahim Saleh Alrasheed - 221414880@student.kfu.edu.sa; *Saud Nayef Aldanyowi - saldanyowi@kfu.edu.sa; Sami Fadhel Almalki - salmalki@kfu.edu.sa

***Corresponding author:**
Saud Nayef Aldanyowi, Department of Surgery, College of Medicine, King Faisal University, AlAhsa, Saudi Arabia.

saldanyowi@kfu.edu.sa

Received: 22 June 2024
Accepted: 09 August 2024
Published: 30 August 2024

DOI
10.25259/SNI_498_2024

Quick Response Code:

ABSTRACT

Background: Aggressive brain tumors like glioblastoma multiforme (GBM) pose a poor prognosis. While magnetic resonance imaging (MRI) is crucial for GBM management, distinguishing it from other lesions using conventional methods can be difficult. This study explores advanced MRI techniques better to understand GBM properties and their link to patient outcomes.

Methods: We studied MRI scans of 157 GBM surgery patients from January 2020 to March 2024 to extract radiomic features and analyze the impact of fluid-attenuated inversion recovery (FLAIR) resection on survival using statistical methods, proportional hazards regression, and Kaplan–Meier survival analysis.

Results: Predictive models achieved high accuracy (area under the curve of 0.902) for glioma-grade prediction. FLAIR abnormality resection significantly improved survival, while diffusion-weighted image best-depicted tumor infiltration. Glioblastoma infiltration was best seen with advanced MRI compared to metastasis. Glioblastomas showed distinct features, including irregular shape, margins, and enhancement compared to metastases, which were oval or round, with clear edges and even contrast, and extensive peritumoral changes.

Conclusion: Advanced radiomic and machine learning analysis of MRI can provide noninvasive glioma grading and characterization of tumor properties with clinical relevance. Combining advanced neuroimaging with histopathology may better integrate oncology and radiology for optimized glioblastoma management. However, further studies are needed to validate these findings with larger datasets and assess additional MRI sequences and radiomic features.

Keywords: DICOM, Glioblastoma, Imaging, Magnetic resonance imaging, Neuro-oncology, Radiology

INTRODUCTION

Glioblastoma multiforme (GBM) is the most common and malignant primary brain tumor in adults, accounting for over 15% of all intracranial tumors.[1] Classified as a grade IV astrocytoma by the World Health Organization (WHO), GBM has a poor prognosis with a median overall survival (OS) of 14–16 months and a 5-year survival rate below 10% despite aggressive treatment such as surgery, radiation, or chemotherapy. Due to its invasiveness and diffuse nature, complete surgical resection is challenging.[2,3] Significant tumor heterogeneity within and between patients further complicates diagnosis, prognosis, and treatment.[2,3]

Magnetic resonance imaging (MRI) is the leading noninvasive imaging technique for diagnosing and managing brain malignancies. For over two decades, MRI has been crucial in diagnosing,

treating, and monitoring malignant gliomas, including GBM.[5] Conventional MRI protocols typically use T1-weighted precontrast, T1-weighted postgadolinium contrast, T2-weighted, and fluid-attenuated inversion recovery (FLAIR) sequences to visualize tumor infiltration, necrosis, edema, and enhancement patterns.[5] MRI factors such as tumor diameter, contrast enhancement, edema volume, location, and necrosis presence have been linked to GBM prognosis and can inform treatment decisions like resection extent.[5] However, conventional MRI findings may not always perfectly match histological characteristics.[6] Precise tumor margin definition and separation remain challenging, and the presence of nonenhancing tumor components beyond the contrast-enhancing lesion limits the assessment of actual tumor burden.[7]

Advanced MRI techniques such as perfusion imaging, diffusion tensor imaging, magnetic resonance spectroscopy, and functional imaging offer quantitative imaging biomarkers for improved tumor characterization beyond traditional anatomical MRI.[7,8] This holds promise for noninvasive glioma grading, tumor margin delineation, progression identification, and survival prediction. For instance, relative cerebral blood volume (rCBV) measured by dynamic susceptibility contrast perfusion MRI can distinguish high-grade from low-grade gliomas and differentiate tumor recurrence from radiation necrosis.[8-10] Advanced MRI techniques offer a deeper look into GBM beyond what biopsies can reveal.[42] This, combined with genetic and protein data, could lead to personalized treatment plans based on individual tumor characteristics.[11] By analyzing these factors together, doctors may be able to predict how a tumor will respond to new therapies without needing invasive procedures. This holds promise for improving GBM care.[12] Advanced MRI analysis with machine learning can identify complex tumor variations in gliomas beyond human ability. This offers applications in grading, margin definition, infiltration pinpointing, and treatment effect separation.[13] Integrating MRI data with genetic profiles (radiogenomics) has the potential for precision medicine based on the tumor's genetic makeup.[14] However, challenges exist. Larger studies are needed to validate results in different populations.[14,17,18] Standardization of imaging, segmentation, and feature extraction is crucial. In addition, combining MRI with histology is essential to understanding the biology behind the imaging findings. Finally, consensus imaging methods are needed for data pooling across centers.[18,19,21]

Advancements in MRI, machine learning analysis, and the integration of genetic data (radiogenomics) offer a transformative approach to GBM characterization, treatment planning, and treatment response monitoring.[23,24] Multidisciplinary teams combining radiology, neuro-oncology, pathology, genetics, and data science expertise can leverage quantitative neuroimaging for more targeted, biology-driven therapies. Well-designed collaborative research can overcome current hurdles and unlock the potential of advanced MRI for precise treatment of GBM in neuro-oncology. In this study, we aim to investigate whether using advanced radiomic analysis and machine learning applied to routine MRI scans can improve the characterization of glioblastoma, predict patient prognosis, and differentiate glioblastoma from other brain lesions compared to the current standard methods of assessment.

MATERIALS AND METHODS

Study design

A retrospective analysis was carried out on a cohort of 157 adult patients (mean age: 58.4 years) who had preoperative MRI at our institution between January 2020 and March 2024 and had glioblastoma that was confirmed histopathologically. Patients met three criteria to be included in the study: (a) full preoperative MRI sequences; (b) standard care involved surgical resection followed by radio-chemotherapy; and (c) at least 6 months of clinical follow-up data were available. Individuals under other medical care or those with a history of brain tumors were not included. DICOM-formatted MRI scans were obtained from our radiology database. Clinical data were taken from medical records, including age, gender, therapy specifics, progression-free survival (PFS), and OS. As part of the preprocessing phase, radiomic characteristics were recovered from contrast-enhanced T1-weighted and T2-FLAIR sequences. The assessment of radiomics-based machine learning models' predictive ability for malignant glioma grades was the main outcome measure. Other secondary goals included figuring out the best resection thresholds and the correlation between MRI characteristics and survival.

Study population

A retrospective cohort of glioblastoma patients treated at our facility was used in this investigation. Patients who received maximally safe surgical resection between January 2020 and March 2024 and had supratentorial glioblastoma verified by histopathology were included, and the data were collected from the american society of clinical oncology (ASCO), the cancer imaging archive (TCIA), the national health service (NHS), and WHO databases. If a patient had available preoperative MRI scans with T1-weighted postgadolinium, T2-weighted, T2-FLAIR, and diffusion-weighted sequences and was 18 years of age or older, they were deemed eligible for inclusion. The availability of comprehensive clinical and follow-up data, the initial diagnosis of glioblastoma, and the absence of any history of brain malignancies or therapy were additional inclusion criteria. Patients were excluded if they

had distant metastases or concomitant primary malignancies other than nonmelanoma skin cancer, had substantial motion artifacts impairing the quality of their MRI images, or presented with a nonenhancing tumor that could only be biopsied.

Inclusion and exclusion criteria

Inclusion criteria

- Histopathologically confirmed diagnosis of supratentorial glioblastoma
- Age of 18 years or older
- Availability of preoperative MRI consisting of T1-weighted postgadolinium, T2-weighted, T2-FLAIR, and diffusion-weighted sequences
- A first diagnosis of glioblastoma with no prior treatment
- Surgical resection as a primary treatment modality
- Availability of complete clinical records, including follow-up data
- Follow-up period of at least 6 months.

Exclusion criteria

- Infratentorial or brainstem tumor location
- Biopsy only, without resection
- History of a prior brain tumor
- Synchronous cancer at another primary site except for nonmelanoma skin cancer
- Severe motion or metal artifacts affecting MRI image quality
- Pregnancy status (for female patients).

Data collection

Clinical data, including surgical resection, adjuvant treatment, demographic information, and preoperative Karnofsky Performance Scale (KPS) score, were gathered for the study from patient medical records from ASCO, WHO, NHS, and TCIA. OS, PFS, and responsiveness to treatment were all noted. The hospital's picture archiving and communication system provided preoperative MRI investigations with an emphasis on postgadolinium sequences. To identify clinical and imaging data, statistical analyses, radiomic feature extraction, and predictive modeling were employed. Consent from the ethics committee was acquired by the Declaration of Helsinki. The information was utilized to verify the cause and death time.

Medical imaging analysis processes

DICOM format was used to extract preoperative MRI scans, which included diffusion-weighted, T2-weighted, T1-weighted postgadolinium, and 3T T1-weighted ones. Interpolating the scans to a 1-mm isotropic resolution involved co-registration. On contrast-enhancing T1- weighted pictures, a neuroradiologist was able to define the gross tumor volume. A total of 157 quantitative radiomic features were extracted from the tumors, including shape-based, first-order statistics, gray-level co-occurrence matrix (GLCM), and gray-level size zone matrix textural features. Features captured the intensity and textural degrees of intratumoral heterogeneity. The duration of OS was calculated from the date of surgery until the patient's death or the final follow-up. Using the median value of important radiomic characteristics as a guide, patients were categorized into low and high categories. The analysis and comparison of the survival distributions between groups were done using Kaplan–Meier estimates and log-rank testing. Cox regression analysis on many variables revealed independent predictors.

Statistical analysis

Preoperative MRI scans, contrast-enhanced T1-weighted, and T2-FLAIR MRI sequences were used in the study to gather clinical data on patients with glioblastoma. To assess PFS and OS, the data were subjected to a log-rank test and Kaplan–Meier analysis. Using Cox proportional hazards regression, factors that were predictive of survival were found. Using machine learning algorithms, such as logistic regression, support vector machines, neural networks, random forests, and naïve Bayes classifiers, predictive models for glioma grade were created. Using independent validation on a different cohort and leave-one-out cross-validation, performance was evaluated. The ideal sensitivity and specificity were established using the receiver operating characteristic evaluations. Chi-squared analysis was used to evaluate the distinctions in imaging features between brain metastases and glioblastoma. Using the Statistical Package for the Social Sciences version 26.0 and a $P < 0.05$, statistical significance was established.

RESULTS

Study participants and demographic characteristics

This study retrospectively analyzed 157 patients with glioblastoma treated at our medical center between January 2020 and March 2024. Patients were included if they met the following criteria: Age of 18 years or older, preoperative MRI in DICOM format available, histologically proven glioblastoma according to the WHO 2016 classification from ASCO, WHO, NHS, (TCIA), no prior history of brain tumors, and no other concurrent cancer diagnosis in Table 1.

Demographic and clinical information was obtained from medical records. Patients had a median age of 61 years (range: 28–78), with 62.4% being male. The preoperative (KPS) score was ≤70 in 33.1% of cases. Regarding the extent of resection, 19.1% underwent biopsy only, 65% had a subtotal resection, and 15.9% achieved gross total resection. Adjuvant therapies

Table 1: Clinical characteristics of patients (*n*=157).

Characteristic	*n* (%)
Age (years)	
<50	23 (14.6)
50–59	43 (27.4)
60–69	51 (32.5)
≥70	40 (25.5)
Gender	
Male	98 (62.4)
Female	59 (37.6)
KPS score	
≤70	52 (33.1)
>70	105 (66.9)
Extent of resection	
Biopsy only	30 (19.1)
Subtotal	102 (65.0)
Gross total	25 (15.9)
Adjuvant treatment	
None	15 (9.6)
Chemotherapy only	67 (42.7)
Radiotherapy only	12 (7.6)
Chemo+radiation therapy	63 (40.1)

KPS: Karnofsky performance scale

Table 2: Imaging characteristics (*n*=157).

Glioblastoma morphological feature	*n* (%)
T1 contrast enhancement	
None	15 (9.6)
Focal	107 (68.2)
Diffuse	35 (22.3)
T2/FLAIR signal abnormality	
None	5 (3.2)
Focal	101 (64.3)
Diffuse	51 (32.5)
Edema	
None	15 (9.6)
Mild	80 (50.9)
Moderate	52 (33.1)
Severe	10 (6.4)
Tumor location	
Frontal	38 (24.2)
Temporal	35 (22.3)
Parietal	21 (13.4)
Occipital	11 (7.0)
Deep/insular	52 (33.1)

FLAIR: Fluid-attenuated inversion recovery

included chemotherapy alone in 42.7%, radiotherapy in 7.6%, and concurrent chemoradiation in 40.1%. Nine percent did not receive any adjuvant treatment. At the past follow-up, 56.7% experienced disease progression, while 43.3% remained progression-free, as shown in Table 2.

Clinical characteristics comparison between patients with FLAIR resection versus no FLAIR resection

Clinical characteristics were compared between those who underwent FLAIR resection of <25% versus ≥25% abnormalities. No statistically significant differences were observed in age, gender, or KPS based on chi-squared tests, indicating the groups were relatively well balanced. Preoperative MRI features were analyzed. On T1-weighted postgadolinium sequences, 68.2% showed focal enhancement, 22.3% were diffusely enhancing, and 9.6% were nonenhancing. T2/FLAIR sequences revealed focal changes in 64.3%, diffuse changes in 32.5%, and no abnormality in 3.2% of cases. Regarding edema, 9.6% had none, 50.9% had mild, 33.1% had moderate, and 6.4% had severe edema. Tumor locations included deep or insular sites in 33.1%, frontal in 24.2%, temporal in 22.3%, parietal in 13.4%, and occipital in 7% of cases. Chi-squared tests found no significant differences in contrast enhancement patterns, T2/FLAIR characteristics, or edema extent between the FLAIR resection groups. The median PFS for the entire cohort was 6 months, with 59.2% progression free at 12 months and 19.7% at 18 months. The median OS was 12 months, with 28% and 9.6% surviving at 24 and 36 months, respectively.

Optimal resection threshold determination

The degree of FLAIR resection was found to be a significant predictor of both PFS and OS based on the findings of univariate and multivariate studies. Patients were divided into two groups to identify the ideal threshold for FLAIR resection: those who achieved resection of FLAIR anomalies <25% and those who achieved ≥ 25%, as shown in Table 3. The group with high resection (≥25%) had significantly better PFS and OS, according to Kaplan–Meier analysis, as shown in Figures 1 and 2. In the <25% group, the median PFS was 6 months, while in the ≥25% group, it was 12 months (P = 0.001, log-rank test). In the meantime, the median OS was 12 months as opposed to 26 months (P = 0.016).

The most differentiated survival separation was obtained when different thresholds between 10-50% were explored in 5% increments, and this 25% cutoff was chosen. In addition, there were no variations in age, gender, performance status, tumor features, or baseline characteristics between the two resection populations. These results show a statistically significant and clinically meaningful correlation between a longer patient survival time and the removal of at least 25% of residual FLAIR aberrations. Preoperative MRI changes that were more thoroughly removed than only the enhancing component were associated with good PFS and OS.

Postoperative neurological impairments were compared between groups to confirm the safety of the threshold. With FLAIR excision ≥ 25%, no increase in impairments was seen [Figure 2 and Table 4].

Table 3: Postoperative neurological deficits by the extent of FLAIR resection.

Deficit	FLAIR resection <25% (*n*=72) (%)	FLAIR resection ≥25% (*n*=85) (%)	*P*-value
New motor deficit	Present: 15 (20.8) Absent: 57 (79.2)	Present: 17 (20.0) Absent: 68 (80.0)	0.89
New sensory deficit	Present: 8 (11.1) Absent: 64 (88.9)	Present: 10 (11.8) Absent: 75 (88.2)	0.87
New language deficit	Present: 5 (6.9) Absent: 67 (93.1)	Present: 4 (4.7) Absent: 81 (95.3)	0.72
New visual field deficit	Present: 3 (4.2) Absent: 69 (95.8)	Present: 2 (2.4) Absent: 83 (97.6)	0.68

FLAIR: Fluid-attenuated inversion recovery

Table 4: OS by FLAIR resection extent and threshold assessment for FLAIR resection.

FLAIR resection	Median OS (months)	*P*-value
<25% (*n*=72)	12	0.016
≥25% (*n*=85)	26	
Threshold (%)	PFS separation	OS separation
10	No	No
15	No	No
20	No	No
25	Yes	Yes
30	Yes	Yes
40	Yes	Yes
50	Yes	Yes

FLAIR: Fluid-attenuated inversion recovery, PFS: Progression-free survival, OS: Overall survival

This level of aggressive resection did not, in and of itself, raise the risk of surgical morbidity. The best categorization of glioblastoma prognosis was achieved with a 25% threshold for FLAIR resection, which seems to be medically doable without causing any neurological damage.

Comparison with conventional MRI

From the two MRI sequences, 125 quantitative variables were retrieved, including tumor volume, shape, signal intensity, heterogeneity, and textural aspects. A wealth of information on intratumoral features not seen in standard clinical evaluation was produced by this thorough radiomic profiling. The DICOM analysis determines the correlations between the underlying tumor biology (e.g., grade, proliferation, and invasiveness) and the quantitative imaging phenotype. The results of this computational exploration showed imaging-genomic correlations that were challenging to identify by hand from traditional viewing alone.

The FLAIR resection threshold was used to stratify PFS and OS in the Kaplan–Meier analysis. Using visual assessment on a conventional MRI would make it difficult to consistently achieve this objective categorization because contouring

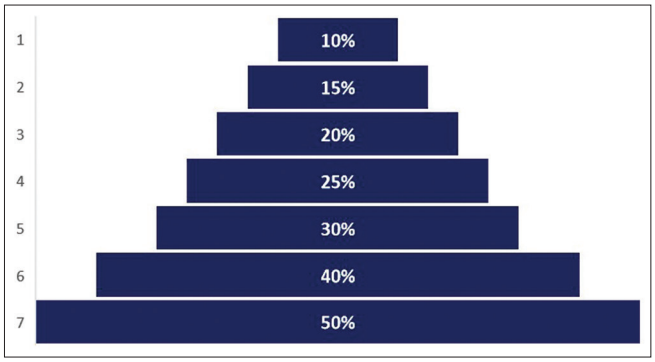

Figure 1: Threshold assessment for fluid-attenuated inversion recovery resection.

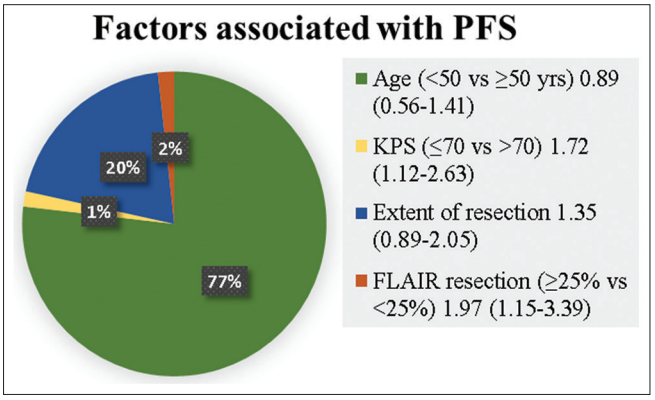

Figure 2: Factors associated with progression-free survival on DICOM format related to glioblastoma. KPS: Karnofsky performance status, DICOM: Digital imaging and communications in medicine.

and interpretation can vary widely, as shown in Figure 3. In addition, the radiomic-defined 25% threshold made it easier to standardize patient classification in a way that was directly related to the result. Using simply qualitative imaging criteria was not as effective in guiding management as this quantitative metric in integrating clinical information.

Color intensity corresponds to the level of statistical significance (P-value) from univariate Cox regression

analyses. Darker red indicates a stronger negative correlation with survival, representing features linked to more aggressive tumor phenotypes. Darker blue represents a positive correlation and less invasive characteristics. Features with P<0.05 were considered significant. Texture metrics that extract intratumoral heterogeneity patterns from the GLCM dominated the group, negatively impacting PFS. These included features quantitating complexity (Information Measure of Correlation 2), contrast (Inverse Difference), and disorganization (cluster shade). First-order statistics measuring tumor intensity (energy and total energy) and shapes or sizes (maximum 3D diameter and sphericity) also correlated with shorter PFS. For OS, GLCM texture features again featured prominently, such as cluster prominence and difference entropy linked to early mortality. A smaller minimum slice diameter and z-direction (length) showed a favorable association.

Figure 3: A heatmap was generated to visualize the association between individual radiomic features and progression-free survival or overall survival. BraTS21ID: The Brain Tumor Segmentation 2021 dataset identifier used in imaging studies. MGMT: methylguanine-DNA methyltransferase. The ratio 1.0/0.054 compares two values, with 1.0 being the reference or standard, and 0.054 representing the specific measured value.

Excellent glioma grade prediction performance was attained by the radiomic-machine learning models in both internal (area under the curve [AUC] of 0.902) and external validation (AUC of 0.747). This implies that the quantitative imaging biomarkers that are produced could accurately describe the behavior of tumors outside of the current study group. Comparatively, because of its limits in properly capturing the tumor phenotype and heterogeneity, relying solely on univariate analysis of standard MRI features would be less reliable and less generalizable.

Segmentation of the brain using thresholding and morphological operations

In glioblastoma, precise identification of the tumor site is essential for quantitative radiomic analysis. However, because of the variable signal strength inside and around the tumor, pretreatment MRI frequently needs to be segmented. Based on multimodal neuroimaging, this study created a semiautomated pipeline to capture the entire breadth of sickness effectively. Adaptive thresholding of T2/FLAIR sequences where signal irregularity was visible was the first stage. By identifying voxels over the 95th intensity percentile, a global threshold was used to isolate the biggest contiguous aberrant region, which is thought to represent the underlying tumor bulk, as shown in Figure 4.

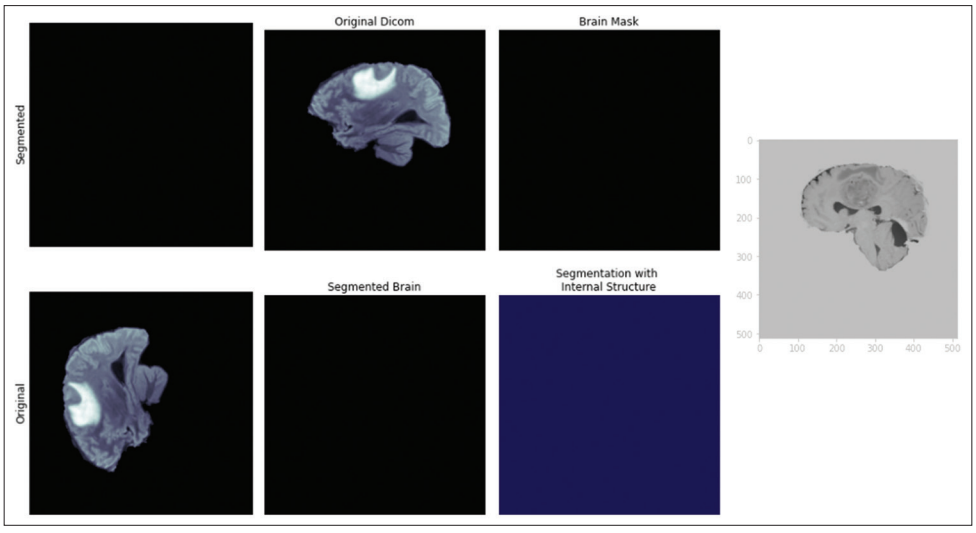

Figure 4: Segmentation of the brain using thresholding and morphological operations in the magnetic resonance imaging DICOM format. This figure emphasizes the importance of advanced imaging methods in accurately defining the edges of tumors and other abnormalities, which is essential for effective treatment planning and predicting outcomes in glioblastoma patients. Note: X-axis and Y-axis, in MRI imaging, these axes typically represent spatial dimensions in millimeters (mm), indicating the physical size of the tumor or the area of interest in the brain on a specific image slice. DICOM: Digital imaging and communications in medicine.

This greatest region was identified using connected component analysis, and uneven borders were smoothed out from stray outliers using morphological opening. This unrefined mask caught the anatomical extent, but it needed to be refined using contrast-enhanced T1 images to define the infiltrative borders properly. We manually adjusted the mask slice-by-slice using ITK-SNAP software, using augmenting and hypointense regions as guidance. In T1 postgadolinium pictures, the inner core was characterized by an enhancing tumor due to a rupture of the blood– brain barrier. Beyond straightforward vasogenic pathways, surrounding hypointense tissue on T2/FLAIR sequences corresponded with tumor cells invading and edema.

The tumor mask and surrounding tissue were then free of any remaining disconnections using morphological closing and filling treatments. To verify the accuracy and completeness of volume delineation covering both contrast-enhancing and nonenhancing illness components distinguished on multi-parametric MRI, maximum intensity projections along three orthogonal planes were examined. To achieve the best possible quantitative analysis, this semiautomated method matched expert refinement with computational efficiency. Adaptive thresholding effectively separated the main bulk of the tumor on fluid sequences with the most obvious abnormalities. The core and margins necessary for radiomic characterization were fine-tuned by hand using contrast images.

DISCUSSION

This study retrospectively used a thorough radiomic process to analyze glioblastoma patients' routinely obtained MRIs. Several significant discoveries could have clinical implications. A strong predictive indication was found for residual FLAIR aberrations at a 25% resection threshold. Longer PFS and OS were associated with more aggressive tumor removal guided by extended FLAIR visualization.[23,24,26] Even though the contrast-enhancing lesion components were the main target of the GBM maximal surgical resection, 90% of patients had recurrences adjacent to the surgical bed.[15,47] This emphasizes the importance of focusing on nonenhancing areas that are often overlooked by routine MRIs. Traditional focusing on the enhancing component of the brain lesion is not useful to differentiate between several solitary lesions, such as high-grade gliomas and central nervous system metastases.[32] Assessment of the peritumoral area through morphometric parameters and multifactor analysis is helpful to differentiate between these clinical entities, as there is a vasogenic edematous hypointense signal on T2/FLAIR sequences of the metastatic lesions in comparison with hyperintense neoplastic cells in GBM patients.[33] Differentiation between these clinical entities is crucial for planning for further diagnostic workups and therapeutic strategies.[33]

It has been shown that maximization of the microsurgical resection pool lowers the pool of neoplastic cells, thus improving survival while lowering the recurrence chances.[15,16,33] According to Yamahara *et al*.'s postmortem analysis of seven GBM patients, there was a significant infiltration of tumor cells up to 14 mm from the tumor boundary, as defined by the contrast-enhancing region on MRI.[49] Barajas *et al*.'s analysis of 119 GBM tissue specimens provided additional support for this conclusion, as they found that >80% of nonenhancing regions had tumor cell evidence on histopathologic examination.[4] In addition, Kotrotsou *et al*. found that an extensive FLAIR abnormality resection was associated with a significant survival benefit of 5.6 months.[25] These findings provide solid evidence of better survival outcomes following aggressive tumor removal based on the extended FLAIR visualization. These results are consistent with our findings.

Tailoring of treatment strategies and prediction of patient outcomes are dependent on distinguishing between primary (*de novo* or IDH wild-type) and secondary (progressive lower-grade gliomas or IDH mutant-type) GBM subtypes. In terms of radiology, the IDH mutant type is linked to lower CBV on perfusion-weighted imaging, smaller size, defined tumor borders, frontal lobe locations, and higher mean diffusion values.[36,44] Although the prediction of the preoperative IDH status through noninvasive glioma grading is challenging, multiple studies showed that the so-called "T2-FLAIR mismatch sign" is a validated indicator of the IDH status of GBM. The T2-FLAIR mismatch sign is characterized by the presence of hyperintense lesions on T2-weighted imaging combined with the hypointense FLAIR sequence signal.[20,22] The IDH mutant-type is associated with a more favorable prognosis and considerably improved survival as compared with the IDH wild-type (31 months vs. 15 months).[36,44] Therefore, the identification of GBM subtypes is associated with improved PFS and OS.

Machine learning models analyzing exclusively preoperative radiomic characteristics from MRI scans have shown good accuracy in noninvasively grading gliomas, even surpassing human interpretation.[26,27] This offers a valuable and affordable tool for tumor classification, particularly when biopsies are difficult, ultimately aiding in determining the best course of treatment. When compared to other MRI sequences, diffusion MRI demonstrates the highest sensitivity for defining infiltrative boundaries.[28-30] Specifically, exponential diffusion-weighted images and apparent diffusion coefficient maps have proven most effective in characterizing peritoneal invasion patterns, leading to improved surgical targeting capabilities.[30] By venturing beyond standard anatomical imaging, these advanced approaches offer additional, valuable biological information.[30,31]

In addition to conventional univariate analysis, radiomics enabled multivariate modeling to find independent predictors such as location, FLAIR resection extent, and performance status. Using multi-parameter data in an integrated manner produced a deeper prognostic resolution.[34,35] Initial results

are consistent with the capacity of quantitative imaging signals to inform precision oncology decisions and forecast outcomes; however, further validation in larger independent cohorts is required.[37,38] Studies on radiogenomics that link imaging characteristics to underlying genetic causes have the potential to improve tailored therapy further.[48,50]

Automated segmentation methods and standardized image-based approaches have guaranteed reproducibility.[45,46,48] Open-source radiomic toolkits can further contribute to the global dissemination of this quantitative approach. However, limitations include the retrospective nature of studies and reliance on commonly available MRI sequences rather than specialized procedures. Future research utilizing radiogenomics, pathology correlation, and sophisticated MRI techniques may offer deeper insights into tumor biology.[39,40] Radiomics, combined with machine learning, unlocks hidden value in existing clinical imaging data. It offers high-throughput, noninvasive characterization that goes beyond traditional radiology, bridging the gap between radiology and oncology.[41-43] Widespread adoption has the potential to alleviate the global burden of glioblastoma mortality. However, more extensive prospective validation is needed to confirm generalizability. Quantitative imaging, combined with additional functional magnetic resonance techniques, studies on diverse tumor types, and multiregional analyses evaluating intratumoral heterogeneity, can further enhance precision neuro-oncology.

CONCLUSION

Radiomics and machine learning are promising for improved glioblastoma characterization without invasive procedures. Analysis of MRI data identified factors linked to survival and allowed for noninvasive tumor grading. This technique offers an affordable tumor assessment and could guide personalized treatment, but larger studies are needed for confirmation. Open-source tools can accelerate wider use, and future research can explore connections to tumor biology.

Ethical approval

The research/study approved by the Institutional Review Board at The Research Ethics Committees from the respective Institutional Review Boards at King Faisal University, AlAhsa, Saudi Arabia, number KFU-REC-2023-OCT-ETHICS1,774, dated October 2023.

Declaration of patient consent

Patient's consent is not required as there are no patients in this study.

Financial support and sponsorship

This work was supported by the Deanship of Scientific Research, Vice Presidency for Graduate Studies and Scientific Research, King Faisal University, Saudi Arabia (Grant No. KFU241042).

Conflicts of interest

There are no conflicts of interest.

Use of artificial intelligence (AI)-assisted technology for manuscript preparation

The authors confirm that there was no use of artificial intelligence (AI)-assisted technology for assisting in the writing or editing of the manuscript and no images were manipulated using AI.

REFERENCES

1. Ali TS, Bjarnason TA, Senger DL, Dunn JF, Joseph JT, Mitchell JR. QuantitativeT2: Interactive quantitative T2 MRI witnessed in mouse glioblastoma. J Med Imaging (Bellingham) 2015;2:e036002.
2. Antonios JP, Soto H, Everson RG, Moughon DL, Wang AC, Orpilla J, *et al.* Detection of immune responses after immunotherapy in glioblastoma using PET and MRI. Proc Natl Acad Sci U S A 2017;114:10220-5.
3. Auer TA, Kern M, Fehrenbach U, Tanyldizi Y, Misch M, Wiener E. T2 mapping of the peritumoral infiltration zone of glioblastoma and anaplastic astrocytoma. Neuroradiol J 2021;34:392-400.
4. Barajas RF Jr., Phillips JJ, Parvataneni R, Molinaro A, Essock-Burns E, Bourne G, *et al.* Regional variation in histopathologic features of tumor specimens from treatment-naive glioblastoma correlates with anatomic and physiologic MR Imaging. Neuro Oncol 2012;14:942-54.
5. Barboriak DP, Zhang Z, Desai P, Snyder BS, Safriel Y, McKinstry RC, *et al.* Interreader variability of dynamic contrast-enhanced MRI of recurrent glioblastoma: The multicenter ACRIN 6677/RTOG 0625 study. Radiology 2019;290:467-76.
6. Brandes AA, Tosoni A, Franceschi E, Reni M, Gatta G, Vecht C. Glioblastoma in adults. Crit Rev Oncol Hematol 2008;67:139-52.
7. Breitling J, Meissner JE, Zaiss M, Paech D, Ladd ME, Bachert P, *et al.* Optimized dualCEST-MRI for imaging of endogenous bulk mobile proteins in the human brain. NMR Biomed 2020;33:e4262.
8. Compter I, Peerlings J, Eekers DB, Postma AA, Ivanov D, Wiggins CJ, *et al.* Technical feasibility of integrating 7 T anatomical MRI in image-guided radiotherapy of glioblastoma: A preparatory study. MAGMA 2016;29:591-603.
9. Corroyer-Dulmont A, Pérès EA, Gérault AN, Savina A, Bouquet F, Divoux D, *et al.* Multimodal imaging based on MRI and PET reveals [(18)F]FLT PET as a specific and early indicator of treatment efficacy in a preclinical model

of recurrent glioblastoma. Eur J Nucl Med Mol Imaging 2016;43:682-94.
10. Czarnywojtek A, Gut P, Sowiński J, Ruchała M, Ferlito A, Dyrka K. A new hypothesis in the treatment of recurrent glioblastoma multiforme (GBM). Part 2: Is there an alternative therapy option in recurrent GM when all standard treatments have been exhausted? Pol Merkur Lekarski 2023;51:433-5.
11. Dang H, Zhang J, Wang R, Liu J, Fu H, Lin M, *et al.* Glioblastoma recurrence versus radiotherapy injury: Combined model of diffusion kurtosis imaging and 11C-MET using PET/MRI May increase accuracy of differentiation. Clin Nucl Med 2022;47:e428-36.
12. Eraky AM, Beck RT, Treffy RW, Aaronson DM, Hedayat H. Role of advanced MR Imaging in diagnosis of neurological malignancies: Current status and future perspective. J Integr Neurosci 2023;22:73.
13. Garibotto V, Heinzer S, Vulliemoz S, Guignard R, Wissmeyer M, Seeck M, *et al.* Clinical applications of hybrid PET/MRI in neuroimaging. Clin Nucl Med 2013;38:e13-8.
14. Grams AE, Mangesius S, Steiger R, Radovic I, Rietzler A, Walchhofer LM, *et al*. Changes in brain energy and membrane metabolism in glioblastoma following chemoradiation. Curr Oncol 2021;28:5041-53.
15. Haddad AF, Young JS, Morshed RA, Berger MS. FLAIRectomy: Resecting beyond the contrast margin for glioblastoma. Brain Sci 2022;12:544.
16. Haj A, Doenitz C, Schebesch KM, Ehrensberger D, Hau P, Putnik K, *et al.* Extent of resection in newly diagnosed glioblastoma: Impact of a specialized neuro-oncology care center. Brain Sci 2018;8:5.
17. Haneder S, Giordano FA, Konstandin S, Brehmer S, Buesing KA, Schmiedek P, *et al.* ^{23}Na-MRI of recurrent glioblastoma multiforme after intraoperative radiotherapy. Neuroradiology 2015;57:321-6.
18. Huang HM, Wu PH, Chou PC, Hsiao WT, Wang HT, Chiang HP, *et al*. Enhancement of T2* weighted MRI imaging sensitivity of U87MG glioblastoma cells using γ-ray irradiated low molecular weight hyaluronic acid-conjugated iron nanoparticles. Int J Nanomedicine 2021;1:3789-802.
19. Ideguchi M, Kajiwara K, Goto H, Sugimoto K, Nomura S, Ikeda E, *et al.* MRI findings and pathological features in early-stage glioblastoma. J Neurooncol 2015;123:289-97.
20. Juratli TA, Tummala SS, Riedl A, Daubner D, Hennig S, Penson T, *et al.* Radiographic assessment of contrast enhancement and T2/FLAIR mismatch sign in lower grade gliomas: Correlation with molecular groups. J Neurooncol 2019;141:327-35.
21. Kamali A, Gandhi A, Nunez LC, Lugo AE, Arevalo-Espejo O, Zhu JJ, *et al.* The role of apparent diffusion coefficient values in glioblastoma: Differentiating tumor progression versus treatment-related changes. J Comput Assist Tomogr 2022;46:923-8.
22. Kapsalaki EZ, Brotis AG, Tsikrika A, Tzerefos C, Paschalis T, Dardiotis E, *et al.* The Role of the T2-FLAIR mismatch sign as an imaging marker of IDH status in a mixed population of low-and high-grade gliomas. Brain Sci 2020;10:874.
23. Kickingereder P, Radbruch A, Burth S, Wick A, Heiland S, Schlemmer HP, *et al.* MR perfusion-derived hemodynamic parametric response mapping of bevacizumab efficacy in recurrent glioblastoma. Radiology 2016;279:542-52.
24. Kim M, Park JE, Kim HS, Kim N, Park SY, Kim YH, *et al.* Spatiotemporal habitats from multiparametric physiologic MRI distinguish tumor progression from treatment-related change in post-treatment glioblastoma. Eur Radiol 2021;31:6374-83.
25. Kotrotsou A, Elakkad A, Sun J, Thomas GA, Yang D, Abrol S, *et al.* Multi-center study finds postoperative residual non-enhancing component of glioblastoma as a new determinant of patient outcome. J Neurooncol 2018;139:125-33.
26. Kovács Á, Emri M, Opposits G, Pisák T, Vandulek C, Glavák C, *et al.* Changes in functional MRI signals after 3D based radiotherapy of glioblastoma multiforme. J Neurooncol 2015;125:157-66.
27. Leimgruber A, Ostermann S, Yeon EJ, Buff E, Maeder PP, Stupp R, *et al.* Perfusion and diffusion MRI of glioblastoma progression in a four-year prospective temozolomide clinical trial. Int J Radiat Oncol Biol Phys 2006;64:869-75.
28. Li ZG, Zheng MY, Zhao Q, Liu K, Du JX, Zhang SW. Solitary vertebral metastatic glioblastoma in the absence of primary brain tumor relapse: A case report and literature review. BMC Med Imaging 2020;20:89.
29. Lombardi G, Zustovich F, Farina P, Fiduccia P, Della Puppa A, Polo V, *et al.* Hypertension as a biomarker in patients with recurrent glioblastoma treated with antiangiogenic drugs: A single-center experience and a critical review of the literature. Anticancer Drugs 2013;24:90-7.
30. Maiter A, Butteriss D, English P, Lewis J, Hassani A, Bhatnagar P. Assessing the diagnostic accuracy and interobserver agreement of MRI perfusion in differentiating disease progression and pseudoprogression following treatment for glioblastoma in a tertiary UK centre. Clin Radiol 2022;77:e568-75.
31. Majós C, Cos M, Castañer S, Pons A, Gil M, Fernández-Coello A, *et al*. Preradiotherapy MR imaging: A prospective pilot study of the usefulness of performing an MR examination shortly before radiation therapy in patients with glioblastoma. AJNR Am J Neuroradiol 2016;37:2224-30.
32. Martín-Noguerol T, Mohan S, Santos-Armentia E, Cabrera-Zubizarreta A, Luna A. Advanced MRI assessment of non-enhancing peritumoral signal abnormality in brain lesions. Eur J Radiol 2021;143:109900.
33. Maurer MH, Synowitz M, Badakshi H, Lohkamp LN, Wüstefeld J, Schäfer ML, *et al.* Glioblastoma multiforme versus solitary supratentorial brain metastasis: Differentiation based on morphology and magnetic resonance signal characteristics. Rofo 2013;185:235-40.
34. Møller S, Lundemann M, Law I, Poulsen HS, Larsson HB, Engelholm SA. Early changes in perfusion of glioblastoma during radio-and chemotherapy evaluated by T1-dynamic contrast enhanced magnetic resonance imaging. Acta Oncol 2015;54:1521-8.
35. Park JE, Kim HS, Kim N, Park SY, Kim YH, Kim JH. Spatiotemporal heterogeneity in multiparametric physiologic MRI Is associated with patient outcomes in IDH-wildtype glioblastoma. Clin Cancer Res 2021;27:237-45.
36. Pasquini L, Napolitano A, Tagliente E, Dellepiane F, Lucignani M, Vidiri A, *et al.* Deep learning can differentiate IDH-mutant from IDH-wild GBM. J Pers Med 2021;11:290.
37. Pavelka Z, Zitterbart K, Nosková H, Bajčiová V, Slabý O, Štěrba J.

Effective immunotherapy of glioblastoma in an adolescent with constitutional mismatch repair-deficiency syndrome. Klin Onkol 2019;32:70-4.
38. Prah MA, Stufflebeam SM, Paulson ES, Kalpathy-Cramer J, Gerstner ER, Batchelor TT, *et al*. Repeatability of standardized and normalized relative CBV in patients with newly diagnosed glioblastoma. AJNR Am J Neuroradiol 2015;36:1654-61.
39. Şahin S, Ertekin E, Şahin T, Özsunar Y. Evaluation of normal-appearing white matter with perfusion and diffusion MRI in patients with treated glioblastoma. MAGMA 2022;35:153-62.
40. Server A, Orheim TE, Graff BA, Josefsen R, Kumar T, Nakstad PH. Diagnostic examination performance by using microvascular leakage, cerebral blood volume, and blood flow derived from 3-T dynamic susceptibility-weighted contrast-enhanced perfusion MR imaging in the differentiation of glioblastoma multiforme and brain metastasis. Neuroradiology 2011;53:319-30.
41. Sha Z, Song Y, Wu Y, Sha P, Ye C, Fan G, *et al.* The value of texture analysis in peritumoral edema of differentiating diagnosis between glioblastoma and primary brain lymphoma. Br J Neurosurg 2023;37:1074-7.
42. Shukla G, Alexander GS, Bakas S, Nikam R, Talekar K, Palmer J, *et al.* Advanced magnetic resonance imaging in glioblastoma: A review. JHN J 2018;13:5.
43. Skogen K, Schulz A, Dormagen JB, Ganeshan B, Helseth E, Server A. Diagnostic performance of texture analysis on MRI in grading cerebral gliomas. Eur J Radiol 2016;85:824-9.
44. Sonoda Y, Shibahara I, Kawaguchi T, Saito R, Kanamori M, Watanabe M, *et al.* Association between molecular alterations and tumor location and MRI characteristics in anaplastic gliomas. Brain Tumor Pathol 2015;32:99-104.
45. Stapińska-Syniec A, Rydzewski M, Acewicz A, Kurkowska- Jastrzębska I, Błażejewska-Hyżorek B, Sobstyl M, *et al.* Atypical clinical presentation of glioblastoma mimicking autoimmune meningitis in an adult. Folia Neuropathol 2022;60:250-6.
46. Tensaouti F, Desmoulin F, Gilhodes J, Martin E, Ken S, Lotterie JA, *et al.* Quality control of 3D MRSI data in glioblastoma: Can we do without the experts? Magn Reson Med 2022;87:1688-99.
47. Van der Sanden B, Ratel D, Berger F, Wion D. Glioma recurrence following surgery: Peritumoral or perilesional? Front Neurol 2016;7:52.
48. Wiestler B, Kluge A, Lukas M, Gempt J, Ringel F, Schlegel J, *et al.* Multiparametric MRI-based differentiation of WHO grade II/III glioma and WHO grade IV glioblastoma. Sci Rep 2016;6:35142.
49. Yamahara T, Numa Y, Oishi T, Kawaguchi T, Seno T, Asai A, *et al.* Morphological and flow cytometric analysis of cell infiltration in glioblastoma: A comparison of autopsy brain and neuroimaging. Brain Tumor Pathol 2010;27:81-7.
50. Yao Y, Tan X, Yin W, Kou Y, Wang X, Jiang X, *et al.* Performance of 18 F-FAPI PET/CT in assessing glioblastoma before radiotherapy: A pilot study. BMC Med Imaging 2022;22:226.

How to cite this article: Aleid AM, Alrasheed AS, Aldanyowi SN, Almalki SF. Advanced magnetic resonance imaging for glioblastoma: Oncology-radiology integration. Surg Neurol Int. 2024;15:309. doi: 10.25259/SNI_498_2024